


# Permafrost thaw with warming reduces microbial metabolic capacities in subsurface soils

Linwei Wu<sup>1</sup>  | Felix Yang<sup>1</sup> | Jiajie Feng<sup>1</sup> | Xuanyu Tao<sup>1</sup> | Qi Qi<sup>2</sup> | Cong Wang<sup>1</sup> | Edward A. G. Schuur<sup>3</sup> | Rosvel Bracho<sup>4</sup> | Yi Huang<sup>5</sup> | James R. Cole<sup>6</sup> | James M. Tiedje<sup>6</sup> | Jizhong Zhou<sup>1,7</sup>

<sup>1</sup>Department of Microbiology and Plant Biology, School of Civil Engineering and Environmental Sciences, Institute for Environmental Genomics, University of Oklahoma, Norman, Oklahoma, USA

<sup>2</sup>School of Environment, State Key Joint Laboratory of Environment Simulation and Pollution Control, Tsinghua University, Beijing, China

<sup>3</sup>Center for Ecosystem Science and Society, Northern Arizona University, Flagstaff, Arizona, USA

<sup>4</sup>Department of Biology, School of Forest Resources and Conservation, University of Florida, Gainesville, Florida, USA

<sup>5</sup>College of Environmental Science and Engineering, State Key Joint Laboratory of Environmental Simulation and Pollution Control, Peking University, Beijing, China

<sup>6</sup>Center for Microbial Ecology, Michigan State University, East Lansing, Michigan, USA

<sup>7</sup>Earth and Environmental Sciences, Lawrence Berkeley National Laboratory, Berkeley, California, USA

## Correspondence

Linwei Wu and Jizhong Zhou, Department of Microbiology and Plant Biology, School of Civil Engineering and Environmental Sciences, Institute for Environmental Genomics, University of Oklahoma, Norman, Oklahoma, USA.  
Emails: linwei.wu-1@ou.edu, jzhou@ou.edu

## Funding information

U.S. Department of Energy, Grant/Award Number: DE-SC0004601 and DE-SC0010715

## Abstract

Microorganisms are major constituents of the total biomass in permafrost regions, whose underlain soils are frozen for at least two consecutive years. To understand potential microbial responses to climate change, here we examined microbial community compositions and functional capacities across four soil depths in an Alaska tundra site. We showed that a 5-year warming treatment increased soil thaw depth by 25.7% ( $p = .011$ ) within the deep organic layer (15–25 cm). Concurrently, warming reduced 37% of bacterial abundance and 64% of fungal abundances in the deep organic layer, while it did not affect microbial abundance in other soil layers (i.e., 0–5, 5–15, and 45–55 cm). Warming treatment altered fungal community composition and microbial functional structure ( $p < .050$ ), but not bacterial community composition. Using a functional gene array, we found that the relative abundances of a variety of carbon (C)-decomposing, iron-reducing, and sulphate-reducing genes in the deep organic layer were decreased, which was not observed by the shotgun sequencing-based metagenomics analysis of those samples. To explain the reduced metabolic capacities, we found that warming treatment elicited higher deterministic environmental filtering, which could be linked to water-saturated time, soil moisture, and soil thaw duration. In contrast, plant factors showed little influence on microbial communities in subsurface soils below 15 cm, despite a 25.2% higher ( $p < .05$ ) aboveground plant biomass by warming treatment. Collectively, we demonstrate that microbial metabolic capacities in subsurface soils are reduced, probably arising from enhanced thaw by warming.

## KEYWORDS

carbon cycling, climate warming, functional microbes, permafrost thaw, tundra

## 1 | INTRODUCTION

Nearly half the world's soil organic carbon (C), estimated to be more than 3000 Pg to a depth of 3 m, is stored in the northern circumpolar permafrost region (Schuur et al., 2008, 2015). Climate warming might promote metabolic rates of soil microbial decomposers in permafrost regions (Schuur et al., 2008). As a result, the permafrost ecosystem has released a substantial amount of greenhouse gases of CO<sub>2</sub>, CH<sub>4</sub>, and N<sub>2</sub>O, which in turn accelerates climate warming (Mackelprang et al., 2016; Xue et al., 2016). In order to better understand future C fate, it is essential to reveal the underlying mechanisms governing soil C dynamics, especially the role of microorganisms.

Recent studies have shown that there is considerable variability in microbial biomass abundance, diversity, and community composition in permafrost regions, owing to large spatial heterogeneity both horizontally and vertically in soil texture, ice, and organic-matter contents (Deng et al., 2015; Jansson & Tas, 2014; Mackelprang et al., 2011). Because of nutrient limitation and longer frozen duration, soil below 15 cm typically exhibits lower microbial biomass, diversity, and metabolic capacities than its topsoil (Jansson & Tas, 2014; Mackelprang et al., 2016). A variety of microbial functional groups have been identified, including acetoclastic methanogens, hydrogenotrophic methanogens, sulphate reducers, and ferric reducers (Jansson & Tas, 2014), which are directly or indirectly related to the microbial decomposition of organic matter that releases greenhouse gases.

Soil thaw in permafrost regions can alter abiotic soil conditions, such as C availability, which in turn affects decomposition rates (Monteux et al., 2018). Atmospheric records and modeling have collectively shown that massive C supply arising from permafrost thaw could be an important source of CO<sub>2</sub> across the vast permafrost regions (Tesi et al., 2016), which is supported by a multiyear permafrost incubation experiment showing that a large amount of labile C is readily mineralized after permafrost thaw (Knoblauch et al., 2013). Nevertheless, the organic C in mineral soils (usually in deep soil depths) may be more recalcitrant to decomposition than in organic soils (usually in shallow soil depths) because of a markedly more aromatic C and lower content of O-alkyl C (Slater & Lawrence, 2013). Therefore, aerobic and anaerobic CO<sub>2</sub> production in thawing permafrost might be lower than recent model estimates, wherein the decreased degradability of mineral soils was not considered (Knoblauch et al., 2013). This controversy emphasizes the need for research to elucidate the mechanisms of microbial degradation of soil C pools in permafrost regions, a prerequisite for accurate quantification of the magnitude of C loss under future climatic scenarios (Woodcroft et al., 2018).

The recent International Panel on Climate Change (IPCC) assessment reports project a continuous trend of global warming in the next decades, which could result in widespread permafrost thaw in Arctic ecosystems (Stocker et al., 2014). To understand potential microbial responses to those climate changes, we set up a study site in the permafrost region of Eight Mile Lake, Alaska, USA, to compare the winter warming treatment to its unwarmed control, as previously

described (Natali et al., 2014). Previously, we found that warming treatment steadily increased both thaw depth and soil moisture over time (Salmon et al., 2016). When soil samples were analysed after 1.5 years of warming treatment, we found that warming significantly altered the metabolic capacities of microbial communities in the topsoil, which was measured by gene abundances related to metabolic pathways (Xue et al., 2016). However, the change was only detected by a functional gene microarray named GeoChip rather than metagenome sequencing (Xue et al., 2016), suggesting that choices of technologies could lead to conflicting observations.

After five years of warming treatment, here we examined microbial community compositions and functional capacities across four soil depths (i.e., 0–5 cm, 5–15 cm, 15–25 cm, and 45–55 cm) in the active layer, which are hereafter referred to as the surface organic layer, the middle organic layer, the deep organic layer, and the mineral layer. In the previous study adopting a metagenomics analysis based on shotgun sequencing, we showed that the relative abundances of functional genes associated with C decomposition and methanogenesis in subsurface soils below 15 cm (referred here as to the deep organic layer and the mineral layer) increased with warming treatment (Johnston et al., 2019). To verify the reliability of the results and extend the research to other soil layers, here we adopted the amplicon sequencing technology of marker genes to analyze the bacterial and fungal communities and quantify their abundances. We also adopted GeoChip to analyse microbial metabolic capacity. Since warming-induced soil thaw creates vertical water flow among different soil layers, our overarching hypothesis is that 5-year warming treatment would significantly alter soil microbial community composition and increase metabolic capacities in subsurface soils, as observed in the metagenomics analysis (Johnston et al., 2019). We also hypothesized that microbial responses varied by soil depths. In addition, recent studies to examine warming effects on soil microbial diversity (Guo et al., 2019), community composition (Guo et al., 2018), and activities (Metcalf, 2017; Xue et al., 2016) have only occasionally considered the community assembly processes classified into deterministic (e.g., environmental selection and competition) and stochastic (e.g., random colonization and drift) processes. Therefore, it remains unknown how warming in Alaska tundra affects the relative importance of ecological processes underlying soil microbial community assembly. We also hypothesize that warming imposes selective pressure, thus decreasing the overall stochasticity.

## 2 | MATERIALS AND METHODS

### 2.1 | Site description

Established in 2008, The CiPEHR project, acronym for the Carbon in Permafrost Experimental Heating Research project, is situated in the northern foothills of the Alaska Range (~670 m elevation, 63°52'59" N, 149°13'32" W) highlighted with discontinuous permafrost and acidic soil that settle on a gentle northeast-facing slope.

The monthly mean temperature of the study site ranges widely from a low of  $-6^{\circ}\text{C}$  in December to a high of  $+15^{\circ}\text{C}$  in July. In 1977–2013, the mean annual air temperature was  $-1.45 \pm 0.25^{\circ}\text{C}$ . The average annual precipitation was  $216 \pm 24$  mm from 2004 to 2013. The soil is classified as a Gelisol, which comprises a 45–65 cm thick organic horizon above a mineral layer composing of a cryoturbated mixture of loess and glacial till. The dominant vegetation is a deciduous shrub *Vaccinium uliginosum* and a tussock-forming sedge *Eriophorum vaginatum*. Permafrost thaw and thermokarst forming have been occurring over recent decades.

## 2.2 | Soil sampling

The soil has been warmed since October 2008 by the aboveground snow layer, which serves as a thermal insulator. To increase the depth of the snow layer, six 1.5-m tall and 8-m long snow fences were installed at the CiPEHR site between the winter warming and control plots in the last week of every September (Figure S1a). Each fence represents a warming-control plot pair. Three blocks, each consisting of two plot pairs, were approximately 100 m from each other with fences placed 5 m apart (Natali et al., 2014). The warmed plot of each snow fence was distributed at the leeward side for 5 m from the fence, while the paired control plot was distributed at the windward side for 8–14 m from the fence. The snow thickness increased from an average of 26 cm in control plots to 104 cm in the warming plots (Natali et al., 2014). To maintain the same soil hydrological and light conditions, the removal of both extra snow and snow fences occurred during March 8–15, which is within early spring before the growing season (May–September). This manipulation prevents additional snow from affecting the moisture as an undesirable side effect.

After five years of winter warming treatment, soil samples were taken from each plot in May 2013 with electric drills, as previously described (Xue et al., 2016). The cores were sliced at depths of 0–5 cm, 5–15 cm, 15–25 cm, and 45–55 cm (Figure S1b). In total, we took three blocks  $\times$  2 plots  $\times$  2 treatments  $\times$  4 depths = 48 samples. Those soil samples were used for analysing microbial community and environmental factors.

## 2.3 | Environmental factors

Soil temperature was automatically measured using CR1000 data loggers with Type-T thermocouples (Campbell Scientific Inc.) at each depth of 5, 10, 20, and 50 cm for every 30 min in each plot. Soil moisture was measured by oven-drying the sampled soil at  $60^{\circ}\text{C}$  until reaching constant weights. Soil thaw depths were measured weekly using a metal probe by pushing through the soil until it reaches the ice. Since aboveground vegetation could affect belowground ecosystem, we measured aboveground plant biomass with a nondestructive point-frame method using a  $60 \times 60$  cm frame with a grid size of  $8 \times 8$  cm to construct 49 grid points, as previously described (Natali et al.,

2012). While the species identity and tissue type were recorded, a rod with 1 mm diameter was placed upright through the grid until it touched the plants at each grid point. After drying at  $60^{\circ}\text{C}$ , soil samples were assembled into combustion tins; C and N content was measured using an ECS 4010 Elemental Analyser (Costech Analytical Technologies). Ecosystem respiration ( $R_{\text{eco}}$ ) and growing season net ecosystem exchange (NEE) were measured by an LI-820 infrared gas analyser (LI-COR Biosciences) coupled to flux chambers as previously described (Natali et al., 2011). For  $R_{\text{eco}}$  measurements, the flux chamber was covered by a dark tarp to exclude photosynthesis. Gross primary productivity (GPP) was calculated as the difference between NEE (positive values defined as C sink) and  $R_{\text{eco}}$ .

## 2.4 | Soil DNA extraction

Soil DNA was extracted via intensive grinding with liquid N and purified with a PowerMax Soil DNA Isolation Kit (MO BIO Laboratories Inc.). DNA quality was assessed by a NanoDrop ND-1000 Spectrophotometer (Thermo Fisher Scientific Inc.) using absorbance ratios of 260/280 and 260/230 nm. DNA was then quantified by Pico Green using a FLUOstar OPTIMA fluorescence plate reader (BMG LabTech Inc.).

## 2.5 | Quantitative PCR

Quantitative PCR (qPCR) was performed to determine the absolute abundance of 16S rRNA gene and fungal Internal transcribed spacer (ITS) region. Universal primers 515F and 806R (Caporaso et al., 2011) were used for targeting the V4 region of the 16S rRNA gene, and universal primers ITS7F and ITS4R (Ihrmark et al., 2012) were used for targeting the fungal ITS region. Triplicate 25- $\mu\text{l}$  reactions were used, which contained 12.5  $\mu\text{l}$  of SsoAdvanced Universal SYBR Green Supermix (Bio-Rad, Hercules), 350 nM of the forward primer, 350 nM of the reverse primer, and 1  $\mu\text{l}$  of DNA template. A thermocycler program of 35 cycles of  $95^{\circ}\text{C}$  for 20 s,  $53^{\circ}\text{C}$  (16S rRNA gene) or  $52^{\circ}\text{C}$  (fungal ITS region) for 25 s, and  $72^{\circ}\text{C}$  for 30 s was performed on an IQ5 Multicolor Real-time PCR Detection System (Bio-Rad). Gene copy numbers were determined by a standard curve constructed either with 16S rRNA gene segment of *E. coli* JM109 competent cells (Agilent Technologies Inc.) ( $R^2$  of the standard curve = 0.9999) or fungal ITS segment of *Saccharomyces cerevisiae* strain 18824 (Leibniz Institute DSMZ) ( $R^2$  of the standard curve = 0.9835) in a TA cloning vector (Promega). For each soil sample, three technical replicates were included for qPCR.

## 2.6 | High-throughput amplicon sequencing and raw data processing

For amplicon sequencing library preparation, primer pairs 515F and 806R (Caporaso et al., 2011) were applied to amplify the

V4 hypervariable region of 16S rRNA gene, and primer pairs ITS7F and ITS4R (Ihrmark et al., 2012) were applied to amplify the fungal ITS region. To avoid bias introduced by long sequencing primers, we used a two-step PCR protocol as previously described (Wu et al., 2017). Both steps used 25  $\mu$ l reactions consisting of 0.25 U of high fidelity AccuPrime Taq DNA polymerase (Life Technologies), 2.5  $\mu$ l of 10 $\times$  PCR buffer II including dNTPs (Life Technologies), 0.4  $\mu$ M of both forward and reverse primers, and 10 ng of DNA template (only for the first PCR step). After the first PCR step, the triplicate products were combined, purified with an Agencourt AMPure XP kit (Beckman Coulter), eluted in 50  $\mu$ l water, and aliquoted into three new PCR tubes (15  $\mu$ l each) as the template for the second PCR step. Because all samples were sequenced together, we used reverse primers linking to a unique barcode sequence for each sample in the second PCR step to differentiate samples. Thermal cycling conditions of PCR were denaturation at 94°C for 1 min, then 10 cycles (the first step) or 20 cycles (the second step) of amplification at 94°C for 20 s, 53°C (16S rRNA genes) or 52°C (ITS) for 25 s, and 68°C for 45 s, followed by a final 10-min extension at 68°C.

Sequencing libraries were prepared according to the MiSeq Reagent Kit Preparation Guide (Illumina), with all samples pooled at equal molarity for 16S rRNA gene or ITS. The combined sample library was diluted to 2 nM, denatured with 0.2 N fresh NaOH, diluted to 300  $\mu$ l and 20 pM by Illumina HT1 buffer, and then mixed with 90  $\mu$ l of 12 pM PhiX, and 210  $\mu$ l of prechilled HT1 buffer. The library (600  $\mu$ l) was then loaded with read 1, read 2, and index sequencing primers on a 500-cycle (2  $\times$  250 paired ends) reagent cartridge and run on a MiSeq benchtop sequencer (Illumina).

Sequences were processed on IEG Sequencing Analysis Pipeline (the Sequencing Analysis Pipeline in ([www.ou.edu/ieg/tools/data-analysis-pipeline](http://www.ou.edu/ieg/tools/data-analysis-pipeline))). Sequences were trimmed using BTRIM with a minimum threshold quality score of 20, a minimum length of 100 bp, and within a 5-bp window size. Forward and reverse reads with at least a 50-bp overlap, and  $\leq$ 5% mismatches were joined using FLASH (Magoč & Salzberg, 2011). After sequences with ambiguous N bases were removed, joined sequences with lengths 245–260 bp for the 16S rRNA gene and 100–450 bp for the ITS region were submitted for chimera removal by U-Chime (Edgar et al., 2011). OTUs were clustered through Uclust at a 97% similarity level (Edgar et al., 2011) and assigned for taxonomies through the RDP classifier (Wang et al., 2007) with a confidence cutoff of 0.5. Singleton sequences were removed. The remaining sequences were randomly resampled to a depth of 34,673 reads per sample for the bacterial 16S rRNA gene and 9,255 reads per sample for the fungal ITS region.

## 2.7 | GeoChip 5.0 analyses and raw data processing

Microbial functional genes were analysed using a microarray-based tool – the 180 K version of GeoChip 5.0 (Agilent Technologies Inc.). This microarray contains 161,961 probes targeting 1447 gene

families, including genes associated with 12 major functional categories, biogeochemical processes of C, N, P, S, and metal cycling (Shi et al., 2019). It also contains 5282 probes targeting 16S rRNA gene sequences as positive controls and 3390 Agilent-Standard negative controls. Before hybridization, 1  $\mu$ g of template DNA was labeled with Cy3 for each sample using random primers, dNTP solution, and Klenow, as previously described (Ma et al., 2019). DNA was then purified with Qiagen QIAquick Kit (Qiagen Inc) and dried using a SpeedVac (ThermoFisher Scientific Inc.). After denaturing, labeled samples were hybridized with GeoChip 5.0 M microarrays at 67°C in the presence of 10% formamide for 24 h. Subsequently, microarrays were washed, dried, and scanned at 100% laser power and photomultiplier tube on an MS200 Nimblegen microarray scanner (Roche Nimblegen Inc.). Scanned images were quantified into signal intensities with Agilent's Data Extraction software. Raw signal intensities were uploaded onto an online pipeline ([www.ou.edu/ieg/tools/data-analysis-pipeline](http://www.ou.edu/ieg/tools/data-analysis-pipeline)) for quality control, normalization, and analyses. We normalized the signal intensity of each detected probe by adjusting relative abundance, removing spots with <2 signal-to-noise ratio or <1.3 signal intensity of background, and removing outliers based on judgments of 2 standard deviations.

## 2.8 | Statistical analyses

Various statistical analyses were performed and carried out via package *vegan* (v.2.3-2) (Oksanen et al., 2013) in R software version 3.2.2 (R Core Team, 2014). Microbial  $\alpha$ -diversity was represented by OTU or functional gene richness.  $\beta$ -diversity was calculated by a dissimilarity matrix using the Bray-Curtis index. Permutational multivariate analysis of variance using distance matrices (PERMANOVA) was used to determine the effects of warming, soil depth, and their interactions on microbial community structure dissimilarity represented by the Bray-Curtis dissimilarity index, using function *adonis* of the *vegan* R package (Dixon, 2003). Partial Mantel tests and canonical correspondence analysis (CCA) were used to link major environmental factors to microbial community structure, using functions *mantel.partial* and *cca* of the *vegan* R package (Dixon, 2003). Pearson's correlation analysis was used to examine the correlation between microbial abundance and environmental factors such as soil moisture and winter soil temperature. To examine the effects of experimental warming on microbial communities and environmental factors, we performed linear mixed models, in which the block was used as a random intercept effect. The *lme4* R package was used to implement linear mixed models (Bates et al., 2014). Wald type II  $\chi^2$  tests were used to calculate the *p*-values from the LMMs using the *car* R package (Fox & Weisberg, 2018). *p*-values were adjusted based on false discovery rate according to multiple comparisons among sites. Unless otherwise stated, values of *p*  $\leq$  .05 are regarded as statistically significant. To disentangle the relative importance of deterministic and stochastic mechanisms underlying community assembly, a null model analysis based on Bray-Curtis metrics was used as previously described (Guo et al., 2018). In

brief, the stochastic ratio was calculated as one minus the proportion of the difference between the observed Bray-Curtis similarity and the null expected similarity divided by the observed similarity, as previously described (Zhou et al., 2014). The stochastic ratio was calculated for warming and control samples in each depth, using the web-based pipeline (<http://ieg3.rccc.ou.edu:8080>; NST method). This index quantifies the relative importance of stochastic processes (e.g., random dispersal and ecological drift) compared to that of deterministic processes (e.g., abiotic filtering and biotic competition).

### 3 | RESULTS

#### 3.1 | Environmental factors

Winter warming treatment significantly ( $p < .05$ ) increased soil temperature by 0.4–0.8°C across four layers, with narrower effects in the deep organic layer and the mineral layer (Table S1). However, warming treatment increased soil temperature of the growing season significantly by 1.0–1.1°C only in the deep organic layer and the mineral layer. Accordingly, warming treatment increased soil thaw depth in May 2013 from  $18.3 \pm 0.4$  to  $23.0 \pm 1.5$  cm (linear mixed model,  $p = .001$ ), which was within the deep organic layer. Duration of annual soil thaw was extended from 104 days to 112 days in the deep organic layer, and from 46 days to 79 days in the mineral layer. Warming treatment also considerably increased aboveground plant biomass and gross primary productivity (GPP). Ecosystem respiration ( $R_{\text{eco}}$ ) was increased for 72.9% ( $p < .05$ ).

#### 3.2 | Microbial abundance

Quantitative PCR (qPCR) was performed to determine the absolute abundance of bacterial 16S rRNA gene and fungal Internal transcribed spacer (ITS) region per dry soil weight. Bacterial abundance was similar across all four depths, with an average of  $3.8 \times 10^7$  copies/g soil (Figure 1). In contrast, fungal abundance steadily decreased with soil depths from  $2.7 \times 10^7$  copies/g dry soil in the surface organic layer to  $1.9 \times 10^6$  copies/g soil in the mineral layer, suggesting that fungal abundance was more affected by soil depths. Warming treatment affected bacterial and fungal abundance for the deep organic layer, in which bacterial abundance was 37% lower, and fungal abundance was 64% lower in the warmed plots than those in the control plots (Figure 1). Therefore, soil thaw with warming treatment imposed an adverse effect on the microbial abundance in the deep organic layer at the time when we collected samples (i.e., May 2013). In contrast, warming increased fungal abundance in the surface organic layer (Figure 1b).

#### 3.3 | Bacterial diversity and composition

A total of 18,722 bacterial OTUs were generated from 3,264,397 raw sequences of 16S rRNA gene amplicons. Among them, 9299 (49.7%) OTUs closely matched to identified taxa at the genus

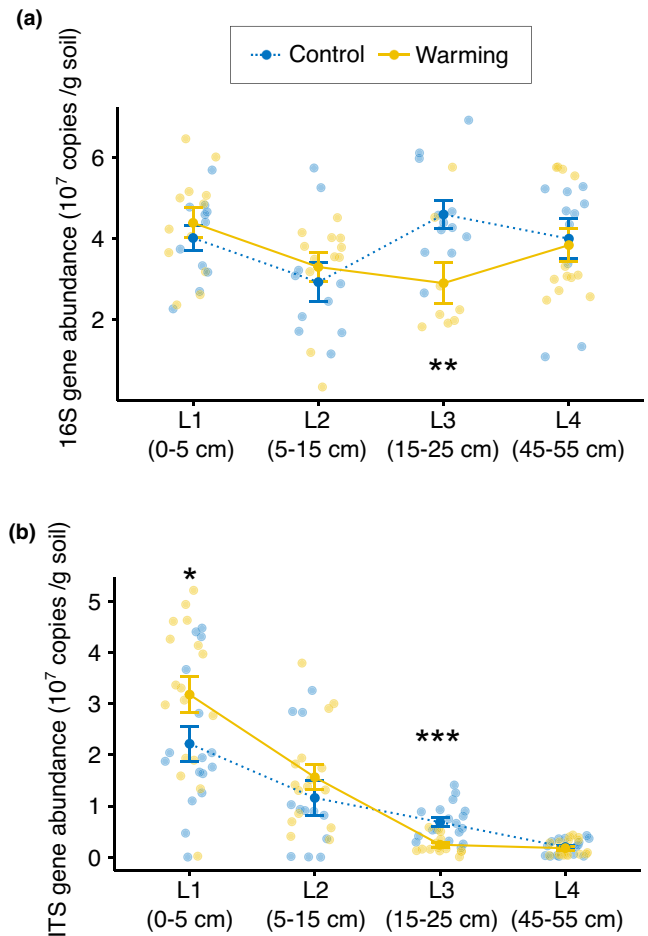


**FIGURE 1** Soil bacterial and fungal abundances measured by qPCR analyses. (a) Bacterial abundance measured by the 16S rRNA gene. (b) Fungal abundance measured by ITS. The difference between warming treatment and control in each layer was examined by the linear mixed model, and statistical significance is based on Wald type II  $\chi^2$  tests, denoting as \*\*\* $p < .001$ , \*\* $p < .01$ , and \* $p < .05$ . Lines represent the mean values, and error bars represent the standard error

level, suggesting that current database coverage of bacterial taxa remains limited in the tundra soil environment. The taxa distribution of bacterial communities fit a lognormal model (Figure S2), showing a long-tail pattern in which the top 167 abundant OTUs (0.89% of the total OTU richness) accounted for 50% of the total sequences. The most abundant phyla included *Acidobacteria*, *Proteobacteria*, and *Actinobacteria* (Table S2). The most abundant OTU was from the *Janibacter* genus, accounting for 1.72% of total sequences. The next four abundant OTUs were related to genera *Bradyrhizobium* (1.54% of total sequences), *Gp3* (1.47% of total sequences), *Pseudolabrys* (1.03% of total sequences), or *Conexibacter* (0.96% of total sequences). Those abundant taxa substantially varied by soil layers. For instance, a *Pseudolabrys* OTU accounted for 3.27% of relative abundance in the mineral layer but dramatically decreased to 0.002% of relative abundance in the surface organic layer.

Notably, the phylum *Dormibacteraeota* accounted for only 0.44% of the sequence abundance in the surface organic layer; however, it increased to 1.61% in the middle organic layer, further increased to 3.28% in the deep organic layer, and decreased to 2.69% in the mineral layer (Table S2). Mantel test and Pearson correlation analysis showed that the top environmental factor linking to *Dormibacteraeota* community composition or abundance was the growing season temperature (Mantel  $r = 0.60$ , adjust  $p = .002$ ; Pearson  $r = -0.51$ , adjust  $p = .001$ ), followed by soil thaw duration, water-saturated time, and soil C/N ratio (Table S3).

Soil depth was a strong factor in determining bacterial community structure, while warming treatment showed no influence (Table 1). Bacterial OTU richness, one of the  $\alpha$ -diversity indices, differed between the middle and deep organic layers, which were largely similar to the results of  $\alpha$ -diversity analyses using indices (Figure S3a). Those diversity indices were highly intercorrelated, suggesting that choices of  $\alpha$ -diversity indices did not affect the results substantially (Figure S4; Pearson  $r = 0.83$ – $0.95$ ,  $p < .001$ ). In addition, the  $\alpha$ -diversity analysis was not affected by sequence depths, as similar results were obtained with a lower sequence depth (Figure S5). Warming treatment also increased the within-treatment bacterial  $\beta$ -diversity in the surface organic layer, the middle organic layer, and the mineral layer (Figure S6a), that is, warming treatment increased community dissimilarity within biological replicates in those three layers.

### 3.4 | Fungal diversity and composition

A total of 2331 fungal OTUs were generated from 1,084,585 raw sequences of the ITS region amplicons. The most abundant phyla were *Ascomycota* and *Basidiomycota*. The most abundant OTU was identified to the family level of *Herpotrichiellaceae*, accounting for 7.7% of total sequences. Although soil depth remained to be the major determinant of fungal community composition, the warming treatment exerted a weaker but significant effect on fungal community composition, suggesting that fungi were more sensitive to warming treatment than bacteria (Table 1). Warming treatment reduced fungal  $\alpha$ -diversity for 55.7% in the mineral layer ( $p = .026$ , Figure S3b) and increased within-treatment fungal  $\beta$ -diversity in the middle and deep organic layers (Figure S6b).

### 3.5 | Microbial functional diversity and composition

We analysed a wide variety of functional genes by GeoChip. In agreement with qPCR, GeoChip analysis revealed that warming

treatment significantly decreased relative abundances of functional genes derived from fungi in the deep organic layer (Figure S7). Functional composition showed a general consistency with the community composition variations derived from the 16S rRNA gene amplicon sequencing data (Mantel test's  $r = 0.46$ ,  $p = .001$ ) and the ITS sequencing data (Mantel test's  $r = 0.53$ ,  $p = .001$ ). Both soil depth ( $F = 13.94$ ,  $p = .001$ ) and the warming treatment ( $F = 3.42$ ,  $p = .009$ ) significantly affected functional community compositions (Table 1). However, functional  $\alpha$ -diversity, calculated by functional gene richness, was similar across all layers (Figure S3c).

### 3.6 | C metabolism genes

The breakdown of high molecular-weight polysaccharides, including starch, cellulose, hemicellulose, lignin, and chitin, is the first stage of C decomposition pertinent to soil C storage (Woodcroft et al., 2018). A total of 9386 GeoChip probes detecting polysaccharide-decomposing genes had positive signals, suggesting that a wide range of microorganisms were responsible for the functionality of C decomposition. Substantially more gene probes were decreased in signal intensity ( $p < .05$ ) than those increased by warming treatment (Figure S8), especially in the middle organic layer and the deep organic layer. Those genes are responsible for decomposing both labile and recalcitrant C. For example, the total signal intensity of genes encoding phenol oxidase for aromatic component decomposition decreased 10.0% in the deep organic layer by warming treatment (Figure 2 and Table S4). Functional genes encoding phospholipase also decreased by 11.0% in the deep organic layer. These results of C metabolism genes were contradictory with what results of the metagenomics analysis (Johnston et al., 2019), which showed that warming treatment increased the relative abundances of genes involved in C decomposition in the deep organic layer.

Fermentation and methanogenesis are of critical concern in thawing permafrost, in which  $\text{CH}_4$  release by monosaccharide decomposition is increasing rapidly (Christensen et al., 2004). Fermentation of ethanol, propionate, acetate, and lactate by reductive tricarboxylic acid cycle is a common metabolism encoded by *Actinobacteria* and *Acidobacteria*, which are particularly abundant in the deep organic layer and the mineral layer (Table S2). We also observed increased relative abundances of fermentative members of *Chloroflexi* (*Anaerolineae*) and *Firmicutes* (*Clostridia*) with increased soil depth, indicating higher fermentation potential in subsurface

Effects	df	Bacteria		Fungi		Functional genes	
		F	p-value	F	p-value	F	p-value
W	1	1.60	.12	1.90	.02	3.42	.009
D	3	20.29	.001	3.68	.001	13.94	.001
W × D	3	1.13	.29	0.90	.71	2.37	.003

TABLE 1 Effects of warming and soil depth on microbial community compositions by PERMANOVA

Abbreviations: D, depth; df, degree of freedom; F, F-statistic value; W, warming.

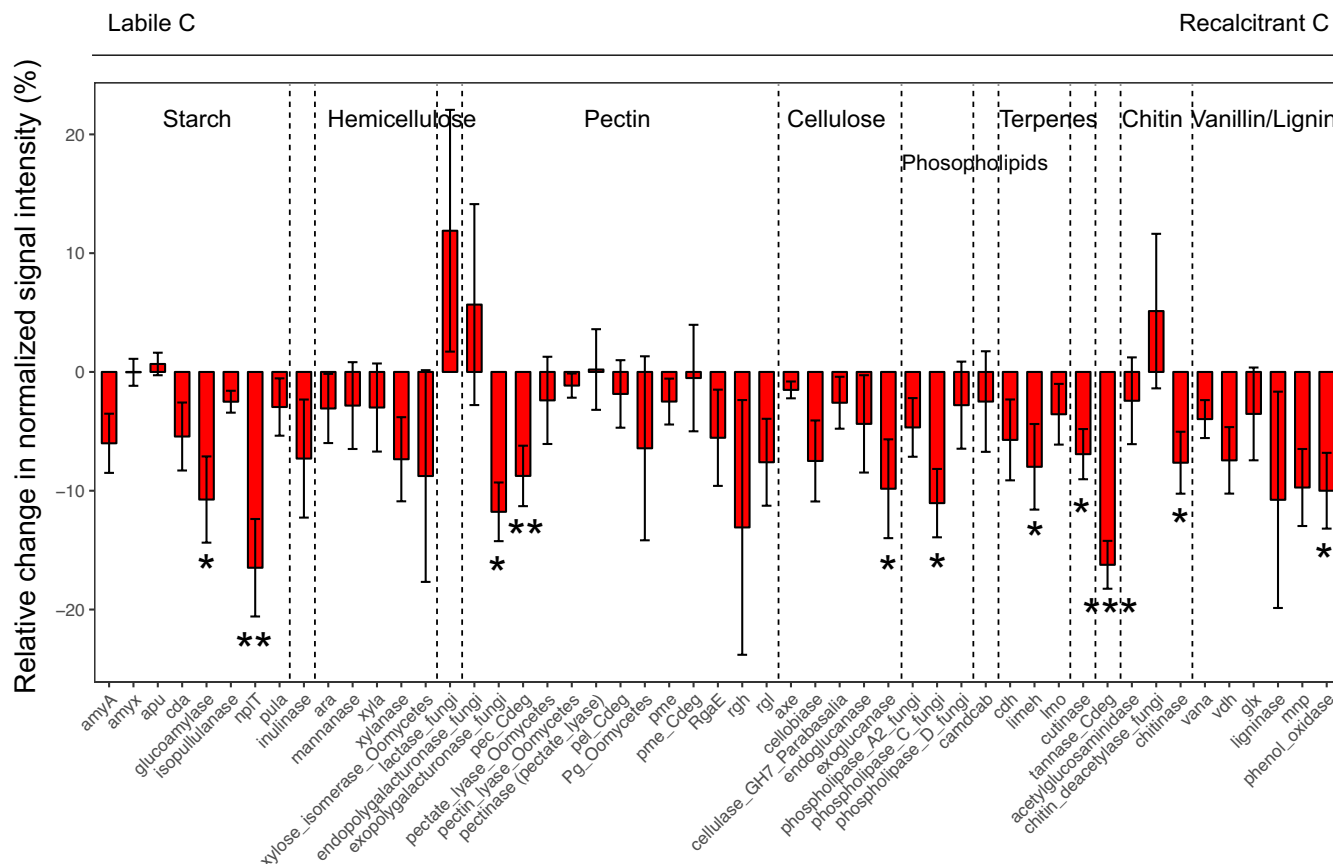


FIGURE 2 Warming effects on C degradation genes in the deep organic layer. The relative changes in the average signal intensity of functional genes by warming treatment are shown. Warming effects were examined by two-tailed *t*-test, and the significance levels are denoted by the asterisks: \*\*\* $p < .001$ , \*\* $p < .01$ , and \* $p < .05$ . Bars represent the mean values, and error bars represent the standard error

soils. For methanogenesis, we examined *mcrA* probes encoding the  $\alpha$ -subunit of methyl coenzyme M reductase, a biomarker of obligate anaerobic methanogenesis, to catalyze the final step in biogenic  $\text{CH}_4$  production. A total of 50 *mcrA* probes measuring the metabolic potential for hydrogenotrophic and acetoclastic methanogens showed positive signals, suggesting this community could utilize both pathways for methanogenesis (Table S5).

### 3.7 | Iron reduction and sulphate reduction

In anoxic permafrost region, iron and sulphate reduction is important for accepting electrons that necessitate fermentation (Mackelprang et al., 2016). However, Fe(III)-reducing genes, such as those encoding *c*-type cytochromes, were decreased substantially ( $p < .05$ ) by warming treatment (Table S6). Cytochromes are iron-containing heme proteins that play a crucial role in metal reduction and electron transfer reactions. This observation coincided with the decreasing trend of C-decomposing genes (Figure 2 and S8), suggesting a potential coupling between Fe(III) reduction and C decomposition.

Many iron cycling and uptake genes were also susceptible to warming treatment (Tables S6 and S7). Those genes included *iuc* encoding an aerobactin siderophore biosynthesis protein from *Vibrio coralliilyticus* ATCC BAA-450 and *Yersinia intermedia* ATCC 29909, which were decreased by warming treatment in both the middle organic layer and the mineral layer ( $p < .03$ , Table S7). Additionally, the heme receptor-encoding gene *hxC* associated with *Haemophilus influenzae* 86-028NP and *Mannheimia haemolytica* serotype A2 str. OVINE also substantially decreased in the deep organic layer ( $p < .03$ ).

Multiple genes involved in sulphate reduction were decreased by warming treatment, especially for the deep organic layer (Tables S6 and S7). For instance, the total signal intensity of *AprA* genes encoding the adenylylsulphate reductase decreased by 18.7% in the deep organic layer. The most susceptible *AprA* genes were those associated with *Desulfobulbus propionicus* DSM 2032, *Thiobacillus plumbophilus*, and an uncultured  $\alpha$ -*Proteobacterium* (Table S7). The *PAPS reductase* gene, which encodes the phosphoadenosine phosphosulphate reductase from *Ustilago maydis* 521, was also decreased in the deep organic layer by warming treatment.

### 3.8 | Ecological processes underlying soil microbial communities

To discern the relative importance of stochastic and deterministic processes in shaping soil community structure, we calculated stochastic ratios based on taxonomic metrics, as previously described (Zhou et al., 2014). For bacterial, fungal, and functional gene compositions, stochastic ratios were consistently <50% (Figure 3), suggesting that deterministic processes could play more important roles in shaping microbial community in the permafrost region. Interestingly, warming treatment significantly ( $p < .05$ ) decreased the relative importance of stochastic processes in shaping bacterial and fungal communities as well as functional gene compositions in the middle organic layer (Figure 3). Warming treatment also decreased the relative importance of stochastic processes in bacterial community assembly in the surface organic layer and fungal community assembly in the deep organic layer. These results indicated that warming treatment could impose significant deterministic effects such as selection on microorganisms.

To unveil the major environmental factors contributing to the deterministic process, we examined linkages between environmental factors and microbial community composition. Water saturated time, soil moisture, and soil thaw duration were the top three environmental factors correlating with both bacterial and fungal community composition (partial Mantel tests, Table 2), followed by soil bulk density, C content, and N content. Those six environmental factors, except for soil bulk density, were also strongly and significantly correlated with functional gene composition. Together with growing season temperature and winter temperature, they explained 34.4% of the variation in the bacterial community composition, 21.4% of the variation in the fungal community composition, and 38.4% of the variation in the functional community composition ( $p < .005$ , CCA, Figure S9). In contrast, plant factors showed little influence on microbial communities in subsurface soils below 15 cm (partial Mantel test, Table S8). For example, plant biomass and GPP were correlated ( $p < .05$ ) with bacterial community composition in the surface organic layer or the middle organic layer, but were not correlated with microbial communities in the deep organic layer or the mineral layer.

## 4 | DISCUSSION

Although research interest in soil microorganisms of permafrost regions has existed for a long time, only over the past decades have we been able to uncover the enormous taxonomic and functional microbial diversity of active layer soils of permafrost regions, paving the road to reveal microbial responses to climate changes. Unexpectedly, our overarching hypothesis that 5-year warming treatment would significantly alter soil microbial community composition and increase metabolic capacities in subsurface soils is only partially supported in this study, since we showed that metabolic capacities in deep organic layer were decreased (Figure 2). Therefore, higher in situ  $\text{CO}_2$  fluxes were unlikely caused by changes in subsurface soil microbial communities, as proposed by Johnston et al. (2019). Rather, microbial biomass (Figure 1) and functional capacity associated with C metabolism in topsoils (Figure S8 and Feng et al., 2020) were increased under warming, which could contribute to the increased  $\text{CO}_2$  fluxes.

### 4.1 | Microbial community composition

Soil depth, rather than warming treatment, significantly affected overall bacterial community composition (Table 1). For example, *Anaerolinea* were abundant across several permafrost regions (Mackelprang et al., 2011). Here, our data of 16S rRNA gene sequences showed that *Anaerolinea* steadily increased from 0.001% in the surface organic layer to 0.009% in the middle organic layer, 0.011% in the deep organic layer, and 1.162% in the mineral layer, despite the insignificant difference between warmed and control plots in this study. Interestingly, the phylum *Dormibacteraeota*, which has no cultured representatives so far (Brewer et al., 2019), was abundant in subsurface soils. As *Dormibacteraeota* appears to adapt to cold and C-depleted environments (Costello, 2007), it might be used as a bioindicator of cold soils because it is highly abundant in much permafrost of Alaska (Tas et al., 2014). Here, we found that the relative abundance of *Dormibacteraeota* showed a very strong negative correlation with soil temperature but not soil C content, suggesting that it might serve as a coldness bioindicator (Table S3). Consistently, the deep organic layer, wherein *Dormibacteraeota* had

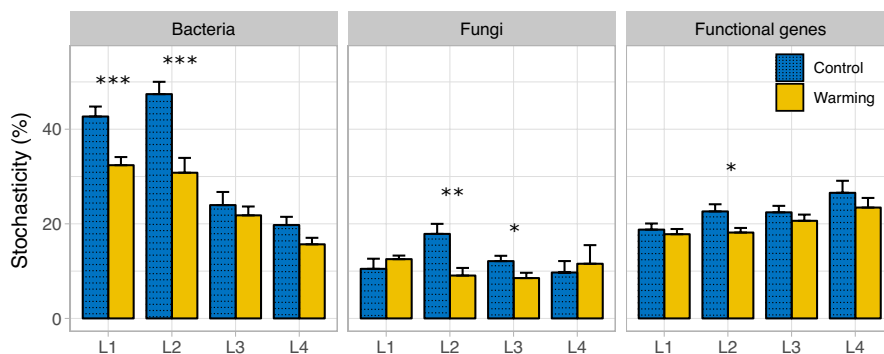


**FIGURE 3** Overall community stochasticity. The significances of the community difference between warming treatment and control are indicated as \*\*\* $p < .001$ , \*\* $p < .01$ , and \* $p < .05$ , based on two-tailed  $t$ -test. Bars represent the mean values, and error bars represent the standard error



**TABLE 2** Partial Mantel tests showing the correlations of dissimilarities of bacterial community composition and those of environmental factors

Environmental factors	Bacteria		Fungi		Functional genes	
	$r_m$	$p$ -value	$r_m$	$p$ -value	$r_m$	$p$ -value
Water saturated time	0.76	.002	0.27	0.007	0.47	.004
Moisture	0.73	.002	0.29	0.007	0.40	.034
Soil thaw duration	0.71	.002	0.28	0.026	0.43	.037
Total C	0.71	.002	0.21	0.039	0.40	.037
Soil bulk density	0.60	.002	0.22	0.056	0.31	.034
Growing season temperature	0.55	.002	0.10	0.115	0.29	.004
Total N	0.51	.002	0.19	0.056	0.31	.004
Winter temperature	0.22	.007	0.12	0.157	0.20	.049
C/N ratio	0.14	.025	0.05	0.364	0.14	.072
Plant biomass	0.25	1	-0.12	0.999	-0.23	1
$R_{eco}$	-0.27	1	-0.19	0.999	-0.22	1
GPP	-0.31	1	-0.16	0.999	-0.23	1
NEE	-0.27	1	-0.01	0.722	-0.16	1

Abbreviations: GPP, average gross primary productivity of the growing season; NEE, average net ecosystem exchange of the growing season;  $R_{eco}$ , average ecosystem respiration of the growing season.

a peak abundance, was only slightly lower in soil C content compared to topsoil. Thus, it is more likely to be a microbial taxon adapted to coldness instead of C limitation.

## 4.2 | Microbial functional capacity

A recent study in a Tibetan alpine grassland showed that five-year in situ warming treatment reduced both soil organic carbon and litter decomposition in the subsurface soil (30–40 cm), as evidenced by lower hydrolase activity and microbial C use efficiency defined as the C partitioning between microbial biomass and respiration (Zhu et al., 2021). However, none of these effects was observed in the topsoil (0–10 cm) of Tibetan grassland (Zhu et al., 2021). Despite the use of completely different technologies, we observed a substantial reduction of bacterial and fungal abundance by warming treatment in the deep organic layer (Figure 1), suggesting that microbial functional capacity, in its absolute value, might be reduced. Additionally, microbial C use efficiency was also decreased by warming (Manzoni et al., 2012). Bacteria have lower biomass C/N ratios than fungi (Keiblinger et al., 2010). When N is limited, bacterial C use efficiency is lower than fungal C use efficiency. Our results showed that fungi abundance was substantially more reduced than bacterial abundance in the deep organic layer by warming treatment (Figure 1), resulting in a smaller fungal/bacterial ratio that was positively correlated with measurements of C use efficiency along with incremental permafrost thaw (Chen et al., 2018). Consequently, warming would result in a high energy cost by restructuring microbial community composition, in addition to elevated metabolic rates (Schuur et al., 2008). The findings of reduced microbial biomass and C-microbial degrading capacity in deep organic layer could alleviate energy spent in respiration.

Although vertical soil profiles are often depicted by dividing into anaerobic zones overlain by aerobic zones, soil systems are more complex in reality, with anaerobic niches found within what would typically be characterized as aerobic zones, and vice versa (Mackelprang et al., 2016). Interestingly, effective indicators of this niche heterogeneity may be given most informatively by microbial data. A diversity of key genes involved in starch, hemicellulose, lignocellulose, and chitin decomposition has been detected in both the active layer and permafrost (Yergeau et al., 2007). We showed that substantially more gene probes associated with C decomposition were decreased in relative abundance than those increased in warming samples (Figure S8), especially in the middle organic layer and the deep organic layer. Unlike our recent metagenomics study showing that relative abundance of genes associated with C decomposition was increased in the deep organic layer (Johnston et al., 2019), our results showed that microbial metabolic capacity could be reduced by warming treatment in the deep organic layer. The distinct results could arise from different methodologies. Although GeoChip has a drawback of only detecting known microorganisms in the sequencing databases (Zhou et al., 2015), the reduction of microbial metabolic capacity revealed by GeoChip was consistent with the qPCR result that warming treatment decreased bacterial abundance by 37% and fungal abundances by 64% lower in the deep organic layer (Figure 1). As discussed in our previous review article (Zhou et al., 2015), differences of GeoChip and metagenomics technologies could result in inconsistent results. For example, our earlier study of 1.5 years warming treatment at the CiPEHR site revealed a significant difference in microbial metabolic capacity between warming and control samples as detected by GeoChip, but not detected by shotgun metagenome sequencing (Xue et al., 2016).

Fermentation was also identified as a prevalent microbial process in an Alaskan permafrost metagenome study (Lipson et al., 2013). Revealed by metagenomics profiling, methanotrophs in a laboratory incubation experiment of permafrost thaw were shown to consume much of  $\text{CH}_4$  despite anaerobic headspace, reflecting aerobic niches from permafrost water or soils (Mackelprang et al., 2011). Here, we detected many *mcrA* genes (Table S5) and methanogen OTUs, suggesting that there was a substantial methanogenesis capacity. The total relative abundance of *mcrA* genes remained unchanged by warming treatment across all soil layers (Table S4), which was similar to a recent study showing that *mcrA* gene copies through quantitative PCR were not changed by warming treatment (Mackelprang et al., 2011). In sharp contrast, another study of *mcrA* gene copies showed a methanogen bloom after thawing in permafrost regions (Wei et al., 2018). Those contradictory results might arise from differences in short-term versus long-term warming effects or high niches heterogeneity in soils. For example, water inundation of microsites creates various C-rich anoxic/anaerobic environments. A high moisture content limits oxygen availability, which stimulates  $\text{CH}_4$  production while suppresses  $\text{CH}_4$  oxidation. Although anaerobic conditions may attenuate total C loss, emission of highly potent  $\text{CH}_4$  in permafrost regions may contribute more to the greenhouse effect than  $\text{CO}_2$  emissions could under aerobic conditions (Mackelprang et al., 2016).

Iron and sulphate reduction capacities have been detected in the active layer and permafrost (Hultman et al., 2015). Concurrently, a large number of genes associated with iron reduction have been detected by metagenomics analysis, suggesting that these processes may be widespread (Lipson et al., 2013). The frequent detection of functional genes associated with iron reduction in our study (Tables S6 and S7) implied that it was an important anaerobic pathway in permafrost regions, though microbial activities related to iron reduction have not been assessed. The sulphate reduction rate at Alaska tundra soil was negligible; it is thus only tractable to evaluate sulphate reduction potentials by functional gene profiling. Based on 16S rRNA gene sequence annotation, sulphate-reducing and sulphur-oxidizing bacteria have been detected in permafrost soils (Mackelprang et al., 2016). Furthermore, functional genes associated with sulphate reduction were more abundant in thawed subsurface soils at depths of 60–100 cm than in undisturbed permafrost soils (Tas et al., 2014). However, our results showed that relative abundances of sulphate reduction genes, as well as iron reduction and C-decomposing genes, were decreased (Table S6), providing further support for high heterogeneity in permafrost regions.

### 4.3 | The ecological drivers underlying soil microbial communities

Quantifying the relative importance of deterministic and stochastic processes in governing community assembly is an important goal in microbial ecology. A previous study showed that metabolites from the permafrost microbiome were reduced by warming, probably as

microbial responses for surviving warming environments (Messan et al., 2020). Using a mathematical framework as statistical proximate (Ning et al., 2019; Zhou et al., 2014), we showed that ecological stochasticity of bacteria, fungi, and functional genes in the organic layer was decreased by warming treatment (Figure 3), suggesting a higher deterministic environmental filtering contributed by intricate abiotic and biotic factors. The deterministic processes could drive the communities to be more similar or dissimilar than random patterns. For example, competition could eliminate more different and less related species that lack certain competitive traits, thus causing communities to be more similar (HilleRisLambers et al., 2012; Mayfield & Levine, 2010). However, competition could also drive the communities to be more dissimilar when closely related species co-occur less than randomly expected due to competitive exclusion (Mayfield & Levine, 2010; Pontarp & Petchey, 2016). The environmental filtering process could also drive communities to be more similar under homogeneous environmental conditions or more dissimilar if the environment is heterogeneous (Ning et al., 2019). We observed increased within-treatment bacterial and fungal  $\beta$ -diversity by warming treatment (Figure S6), which might result from competitive exclusion or heterogeneous environment selection. Consistent with our finding, warming also induced environmental filtering in a tallgrass prairie site of Oklahoma, USA (Guo et al., 2018). Further, we found that warming had different effects on the stochasticity of bacterial, fungal, and functional gene communities in different layers (Figure 3), which might be due to their difference in sensitivity to environmental changes. Microbial functional gene composition (i.e., functional  $\beta$ -diversity) is decoupled from the taxonomy (Louca et al., 2016; Yang, 2021), which explains that warming decreased the stochasticity of bacterial or fungal communities in the surface or deep organic layer, but did not change the stochasticity of functional genes.

Several studies showed that Arctic soil microbial communities responded slowly to warming treatments (Geml et al., 2015; Morgado et al., 2015). Both the composition and functional capacity of bacterial and fungal communities were changed by warming treatment, but only after more than a decade. The most pronounced effects of warming treatment were recorded in water-saturated field sites, underlining the importance of water in determining microbial responses to warming treatment (Walker et al., 2008). Such water-dependent responses were also observed in the fungal community of Arctic soils (Geml et al., 2015). In accordance, we found that water-saturated time, soil moisture, and soil thaw duration were the most important environmental factors correlating with both bacterial and fungal community composition, while GPP appeared not to be important (Table 2). Consequently, water table dynamics may explain summer  $\text{CO}_2$  flux variations across treatments at our study site (Mauritz et al., 2017). In a changing Arctic climate with both warmer air temperatures and greater snowfall, water can become increasingly important in regulating warming effects on microbial communities and C-decomposing rates (Christiansen et al., 2017). Contradictory to model prediction that increased GPP in Arctic ecosystems by climate warming may

offset C loss (Oberbauer et al., 2007), landscape trends toward greater Arctic C loss have been observed (Belshe et al., 2013). The underestimation of C balance may arise from failure to account for continued exposure of organic soil C to microbial communities as permafrost thaws. Additionally, warming-induced soil thaw affects soil moisture and vegetation (Jansson & Tas, 2014), which have not yet been firmly linked to microbial responses (Mackelprang et al., 2016; Monteux et al., 2018).

## 5 | CONCLUSIONS

C decomposition and greenhouse gas emission in thawing permafrost regions operate primarily through microbial functions such as enzyme production, electron transfer, C and nutrient assimilation, and growth. Therefore, functional traits can be used to understand the community-level responses of microorganisms by measuring community composition and metabolic potential (Green et al., 2008). Increasing global efforts have recognized the urgent need to understand the microbial ecology of permafrost. However, our ability to predict responses of permafrost regions to a warming world is limited, partially owing to lack of a clear understanding of microbe-environment interaction and dynamics. As a consequence, the future fate of permafrost C depends critically on microbial abundance, diversity, metabolic capacity, and activities for C decomposition, which are highly uncertain to which extent that climate warming induces greenhouse gas emission. By applying cutting-edge environmental genomics techniques, here we fill the important knowledge gap by uncovering how key members of the permafrost microbial community and their metabolic capacities could potentially respond to climate changes.

## ACKNOWLEDGEMENTS

This work was supported by the United States Department of Energy, Biological Systems Research on the Role of Microbial Communities in Carbon Cycling Program (DE-SC0004601 and DE-SC0010715), DOE Terrestrial Ecosystems Program, NSF LTER program, State Key Joint Laboratory of Environment Simulation and Pollution Control (17L03ESPC), and the Office of the Vice President for Research at the University of Oklahoma.

## AUTHOR CONTRIBUTIONS

Jizhong Zhou, Edward A.G. Schuur, James M. Tiedje, and James R. Cole developed the original concepts. Rosvel Bracho collected soil samples. Jiajie Feng, Xuanyu Tao and Cong Wang extracted DNA, carried out 16S rRNA gene and ITS amplicon sequencing experiments, qPCR experiments and GeoChip microarray experiments. Linwei Wu, Felix Yang, Jiajie Feng, Cong Wang and Qi Qi processed the data of amplicon sequences. Linwei Wu and Felix Yang performed statistical analyses. Linwei Wu, Felix Yang and Jizhong Zhou wrote the manuscript. All authors were given the opportunity to review the results and comment on the manuscript.

## CONFLICT OF INTEREST

The authors declare no conflict of interests.

## DATA AVAILABILITY STATEMENT

Raw sequences of 16S rRNA and ITS amplicon genes have been made available in the NCBI SRA database ([www.ncbi.nlm.nih.gov/sra](http://www.ncbi.nlm.nih.gov/sra)) under accession number PRJNA506455. Raw data of GeoChip experiments can be accessed through the URL (129.15.40.254/NewIEGWebsiteFiles/publications/SupplData/CiPEHR\_JiajieFENG\_Raw\_GeoChip\_Data.txt) and (129.15.40.254/NewIEGWebsiteFiles/publications/SupplData/CiPEHR\_JiajieFENG\_Normalized\_GeoChip\_Data.txt). Metadata are stored in the SRA (BioProject PRJNA506455).

## ORCID

Linwei Wu  <https://orcid.org/0000-0002-6649-5072>

## REFERENCES

- Bates, D., Mächler, M., Bolker, B., & Walker, S. (2014). Fitting linear mixed-effects models using lme4. *arXiv preprint arXiv:1406.5823*.
- Belshe, E., Schuur, E., & Bolker, B. (2013). Tundra ecosystems observed to be CO<sub>2</sub> sources due to differential amplification of the carbon cycle. *Ecology Letters*, 16(10), 1307–1315.
- Brewer, T. E., Aronson, E. L., Arogyaswamy, K., Billings, S. A., Botthoff, J. K., Campbell, A. N., Dove, N. C., Fairbanks, D., Gallery, R. E., Hart, S. C., Kaye, J., King, G., Logan, G., Lohse, K. A., Maltz, M. R., Mayorga, E., O'Neill, C., Owens, S. M., Packman, A., ... Fierer, N. (2019). Ecological and genomic attributes of novel bacterial taxa that thrive in subsurface soil horizons. *bioRxiv*, 10, 647651. <https://doi.org/10.1128/mBio.01318-19>
- Caporaso, J. G., Lauber, C. L., Walters, W. A., Berg-Lyons, D., Lozupone, C. A., Turnbaugh, P. J., Fierer, N., & Knight, R. (2011). Global patterns of 16S rRNA diversity at a depth of millions of sequences per sample. *Proceedings of the National Academy of Sciences*, 108(Supplement 1), 4516–4522. <https://doi.org/10.1073/pnas.1000080107>
- Chen, L., Liu, L. I., Mao, C., Qin, S., Wang, J., Liu, F., Blagodatsky, S., Yang, G., Zhang, Q., Zhang, D., Yu, J., & Yang, Y. (2018). Nitrogen availability regulates topsoil carbon dynamics after permafrost thaw by altering microbial metabolic efficiency. *Nature Communications*, 9(1), 3951. <https://doi.org/10.1038/s41467-018-06232-y>
- Christensen, T. R., Johansson, T., Åkerman, H. J., Mastepanov, M., Malmer, N., Friberg, T., & Svensson, B. H. (2004). Thawing sub-arctic permafrost: Effects on vegetation and methane emissions. *Geophysical Research Letters*, 31(4), L04501. <https://doi.org/10.1029/2003GL018680>
- Christiansen, C. T., Haugwitz, M. S., Priemé, A., Nielsen, C. S., Elberling, B. O., Michelsen, A., Grogan, P., & Blok, D. (2017). Enhanced summer warming reduces fungal decomposer diversity and litter mass loss more strongly in dry than in wet tundra. *Global Change Biology*, 23(1), 406–420. <https://doi.org/10.1111/gcb.13362>
- Costello, E. K. (2007). *Molecular phylogenetic characterization of high altitude soil microbial communities and novel, uncultivated bacterial lineages*. University of Colorado at Boulder.
- Deng, J., Gu, Y., Zhang, J., Xue, K., Qin, Y., Yuan, M., & Zhou, J. (2015). Shifts of tundra bacterial and archaeal communities along a permafrost thaw gradient in Alaska. *Molecular Ecology*, 24(1), 222–234.
- Dixon, P. (2003). VEGAN, a package of R functions for community ecology. *Journal of Vegetation Science*, 14(6), 927–930. <https://doi.org/10.1111/j.1654-1103.2003.tb02228.x>

- Edgar, R. C., Haas, B. J., Clemente, J. C., Quince, C., & Knight, R. (2011). UCHIME improves sensitivity and speed of chimera detection. *Bioinformatics*, 27(16), 2194–2200. <https://doi.org/10.1093/bioinformatics/btr381>
- Feng, J., Wang, C., Lei, J., Yang, Y., Yan, Q., Zhou, X., Tao, X., Ning, D., Yuan, M. M., Qin, Y., Shi, Z. J., Guo, X., He, Z., Van Nostrand, J. D., Wu, L., Bracho-Garillo, R. G., Penton, C. R., Cole, J. R., Konstantinidis, K. T., ... Zhou, J. (2020). Warming-induced permafrost thaw exacerbates tundra soil carbon decomposition mediated by microbial community. *Microbiome*, 8(1), 1–12. <https://doi.org/10.1186/s40168-019-0778-3>
- Fox, J., & Weisberg, S. (2018). *An R companion to applied regression*. Sage Publications.
- Geml, J., Morgado, L. N., Semenova, T. A., Welker, J. M., Walker, M. D., & Smets, E. (2015). Long-term warming alters richness and composition of taxonomic and functional groups of arctic fungi. *FEMS Microbiology Ecology*, 91(8), fiv095. <https://doi.org/10.1093/femsec/fiv095>
- Green, J. L., Bohannan, B. J., & Whitaker, R. J. (2008). Microbial biogeography: from taxonomy to traits. *Science*, 320(5879), 1039–1043.
- Guo, X., Feng, J., Shi, Z., Zhou, X., Yuan, M., Tao, X., Hale, L., Yuan, T., Wang, J., Qin, Y., Zhou, A., Fu, Y., Wu, L., He, Z., Van Nostrand, J. D., Ning, D., Liu, X., Luo, Y., Tiedje, J. M., ... Zhou, J. (2018). Climate warming leads to divergent succession of grassland microbial communities. *Nature Climate Change*, 8(9), 813–818. <https://doi.org/10.1038/s41558-018-0254-2>
- Guo, X., Zhou, X., Hale, L., Yuan, M., Ning, D., Feng, J., Shi, Z., Li, Z., Feng, B., Gao, Q., Wu, L., Shi, W., Zhou, A., Fu, Y., Wu, L., He, Z., Van Nostrand, J. D., Qiu, G., Liu, X., ... Zhou, J. (2019). Climate warming accelerates temporal scaling of grassland soil microbial biodiversity. *Nature Ecology & Evolution*, 3(4), 612–619. <https://doi.org/10.1038/s41559-019-0848-8>
- HilleRisLambers, J., Adler, P. B., Harpole, W. S., Levine, J. M., & Mayfield, M. M. (2012). Rethinking community assembly through the lens of coexistence theory. *Annual Review of Ecology, Evolution, and Systematics*, 43, 227–248. <https://doi.org/10.1146/annurev-ecolsys-110411-160411>
- Hultman, J., Waldrop, M. P., Mackelprang, R., David, M. M., McFarland, J., Blazewicz, S. J., & Shah, M. B. (2015). Multi-omics of permafrost, active layer and thermokarst bog soil microbiomes. *Nature*, 521(7551), 208–212.
- Ihrmark, K., Bodeker, I. T. M., Cruz-Martinez, K., Friberg, H., Kubartova, A., Schenck, J., Strid, Y., Stenlid, J., Brandström-Durling, M., Clemmensen, K. E., & Lindahl, B. D. (2012). New primers to amplify the fungal ITS2 region—evaluation by 454-sequencing of artificial and natural communities. *FEMS Microbiology Ecology*, 82(3), 666–677. <https://doi.org/10.1111/j.1574-6941.2012.01437.x>
- Jansson, J. K., & Tas, N. (2014). The microbial ecology of permafrost. *Nature Reviews Microbiology*, 12(6), 414–425. <https://doi.org/10.1038/nrmicro3262>
- Johnston, E. R., Hatt, J. K., He, Z., Wu, L., Guo, X., Luo, Y., Schuur, E. A. G., Tiedje, J. M., Zhou, J., & Konstantinidis, K. T. (2019). Responses of tundra soil microbial communities to half a decade of experimental warming at two critical depths. *Proceedings of the National Academy of Sciences*, 116(30), 15096–15105. <https://doi.org/10.1073/pnas.1901307116>
- Keibinger, K. M., Hall, E. K., Wanek, W., Szukics, U., Hämmerle, I., Ellersdorfer, G., Böck, S., Strauss, J., Sterflinger, K., Richter, A., & Zechmeister-Boltenstern, S. (2010). The effect of resource quantity and resource stoichiometry on microbial carbon-use efficiency. *FEMS Microbiology Ecology*, 73(3), 430–440. <https://doi.org/10.1111/j.1574-6941.2010.00912.x>
- Knoblauch, C., Beer, C., Sosnin, A., Wagner, D., & Pfeiffer, E. M. (2013). Predicting long-term carbon mineralization and trace gas production from thawing permafrost of Northeast Siberia. *Global Change Biology*, 19(4), 1160–1172. <https://doi.org/10.1111/gcb.12116>
- Lipson, D. A., Haggerty, J. M., Srinivas, A., Raab, T. K., Sathe, S., & Dinsdale, E. A. (2013). Metagenomic insights into anaerobic metabolism along an Arctic peat soil profile. *PLoS One*, 8(5), e64659. <https://doi.org/10.1371/journal.pone.0064659>
- Louca, S., Parfrey, L. W., & Doebeli, M. (2016). Decoupling function and taxonomy in the global ocean microbiome. *Science*, 353(6305), 1272–1277.
- Ma, X., Zhang, Q., Zheng, M., Gao, Y., Yuan, T., Hale, L., Van Nostrand, J. D., Zhou, J., Wan, S., & Yang, Y. (2019). Microbial functional traits are sensitive indicators of mild disturbance by lamb grazing. *ISME Journal*, 13(5), 1370–1373. <https://doi.org/10.1038/s41396-019-0354-7>
- Mackelprang, R., Saleska, S. R., Jacobsen, C. S., Jansson, J. K., & Taş, N. (2016). Permafrost meta-omics and climate change. *Annual Review of Earth and Planetary Sciences*, 44(1), 439–462. <https://doi.org/10.1146/annurev-earth-060614-105126>
- Mackelprang, R., Waldrop, M. P., DeAngelis, K. M., David, M. M., Chavarria, K. L., Blazewicz, S. J., Rubin, E. M., & Jansson, J. K. (2011). Metagenomic analysis of a permafrost microbial community reveals a rapid response to thaw. *Nature*, 480, 368–371. <https://doi.org/10.1038/nature10576>
- Magoč, T., & Salzberg, S. L. (2011). FLASH: fast length adjustment of short reads to improve genome assemblies. *Bioinformatics*, 27(21), 2957–2963. <https://doi.org/10.1093/bioinformatics/btr507>
- Manzoni, S., Taylor, P., Richter, A., Porporato, A., & Ågren, G. I. (2012). Environmental and stoichiometric controls on microbial carbon-use efficiency in soils. *New Phytologist*, 196(1), 79–91. <https://doi.org/10.1111/j.1469-8137.2012.04225.x>
- Mauritz, M., Bracho, R., Celis, G., Hutchings, J., Natali, S. M., Pegoraro, E., & Schuur, E. A. G. (2017). Nonlinear CO<sub>2</sub> flux response to 7 years of experimentally induced permafrost thaw. *Global Change Biology*, 23(9), 3646–3666.
- Mayfield, M. M., & Levine, J. M. (2010). Opposing effects of competitive exclusion on the phylogenetic structure of communities. *Ecology Letters*, 13(9), 1085–1093. <https://doi.org/10.1111/j.1461-0248.2010.01509.x>
- Messan, K. S., Jones, R. M., Doherty, S. J., Foley, K., Douglas, T. A., & Barbato, R. A. (2020). The role of changing temperature in microbial metabolic processes during permafrost thaw. *PLoS One*, 15(4), e0232169. <https://doi.org/10.1371/journal.pone.0232169>
- Metcalfe, D. B. (2017). Microbial change in warming soils. *Science*, 358(6359), 41–42.
- Monteux, S., Weedon, J. T., Blume-Werry, G., Gavazov, K., Jassey, V. E. J., Johansson, M., Keuper, F., Olid, C., & Dorrepaal, E. (2018). Long-term in situ permafrost thaw effects on bacterial communities and potential aerobic respiration. *ISME Journal*, 12(9), 2129–2141. <https://doi.org/10.1038/s41396-018-0176-z>
- Morgado, L. N., Semenova, T. A., Welker, J. M., Walker, M. D., Smets, E., & Geml, J. (2015). Summer temperature increase has distinct effects on the ectomycorrhizal fungal communities of moist tussock and dry tundra in Arctic Alaska. *Global Change Biology*, 21(2), 959–972. <https://doi.org/10.1111/gcb.12716>
- Natali, S. M., Schuur, E. A. G., & Rubin, R. L. (2012). Increased plant productivity in Alaskan tundra as a result of experimental warming of soil and permafrost. *Journal of Ecology*, 100(2), 488–498. <https://doi.org/10.1111/j.1365-2745.2011.01925.x>
- Natali, S. M., Schuur, E. A., Trucco, C., Pries, C. E. H., Crummer, K. G., & Lopez, A. F. B. (2011). Effects of experimental warming of air, soil and permafrost on carbon balance in Alaskan tundra. *Global Change Biology*, 17(3), 1394–1407. <https://doi.org/10.1111/j.1365-2486.2010.02303.x>
- Natali, S. M., Schuur, E. A., Webb, E. E., Pries, C. E. H., & Crummer, K. G. (2014). Permafrost degradation stimulates carbon loss from experimentally warmed tundra. *Ecology*, 95(3), 602–608. <https://doi.org/10.1890/13-0602.1>
- Ning, D., Deng, Y., Tiedje, J. M., & Zhou, J. (2019). A general framework for quantitatively assessing ecological stochasticity. *Proceedings of*

- the National Academy of Sciences, 116(34), 16892–16898. <https://doi.org/10.1073/pnas.1904623116>
- Oberbauer, S. F., Tweedie, C. E., Welker, J. M., Fahnestock, J. T., Henry, G. H., Webber, P. J., & Elmore, E. (2007). Tundra CO<sub>2</sub> fluxes in response to experimental warming across latitudinal and moisture gradients. *Ecological Monographs*, 77(2), 221–238.
- Oksanen, J., Blanchet, F. G., Kindt, R., Legendre, P., Minchin, P. R., O'hara, R., & Wagner, H. (2013). Package 'vegan'. Community Ecology Package Version 2(9). <https://cran.r-project.org/>; <https://github.com/vegandevs/vegan>
- Pontarp, M., & Petchey, O. L. (2016). Community trait overdispersion due to trophic interactions: concerns for assembly process inference. *Proceedings of the Royal Society B: Biological Sciences*, 283(1840), 20161729.
- R Core Team (2014). *R: A language and environment for statistical computing*. R Foundation for Statistical Computing.
- Salmon, V. G., Soucy, P., Mauritz, M., Celis, G., Natali, S. M., Mack, M. C., & Schuur, E. A. (2016). Nitrogen availability increases in a tundra ecosystem during five years of experimental permafrost thaw. *Global Change Biology*, 22(5), 1927–1941. <https://doi.org/10.1111/gcb.13204>
- Schuur, E. A. G., Bockheim, J., Canadell, J. G., Euskirchen, E., Field, C. B., Goryachkin, S. V., Hagemann, S., Kuhry, P., Laflour, P. M., Lee, H., Mazhitova, G., Nelson, F. E., Rinke, A., Romanovsky, V. E., Shiklomanov, N., Tarnocai, C., Venevsky, S., Vogel, J. G., & Zimov, S. A. (2008). Vulnerability of permafrost carbon to climate change: Implications for the global carbon cycle. *BioScience*, 58(8), 701–714. <https://doi.org/10.1641/B580807>
- Schuur, E. A., McGuire, A. D., Schädel, C., Grosse, G., Harden, J., Hayes, D. J., & Lawrence, D. M. (2015). Climate change and the permafrost carbon feedback. *Nature*, 520(7546), 171–179.
- Shi, Z., Yin, H., Van Nostrand, J. D., Voordeckers, J. W., Tu, Q., Deng, Y. E., Yuan, M., Zhou, A., Zhang, P., Xiao, N., Ning, D., He, Z., Wu, L., & Zhou, J. (2019). Functional gene array-based ultrasensitive and quantitative detection of microbial populations in complex communities. *Msystems*, 4(4), e00296-19. <https://doi.org/10.1128/mSystems.00296-19>
- Slater, A. G., & Lawrence, D. M. (2013). Diagnosing present and future permafrost from climate models. *Journal of Climate*, 26(15), 5608–5623. <https://doi.org/10.1175/JCLI-D-12-00341.1>
- Stocker, T. F., Qin, D., Plattner, G.-K., Tignor, M. M., Allen, S. K., Boschung, J., & Midgley, P. M. (2014). *Climate Change 2013: The physical science basis contribution of working group I to the fifth assessment report of IPCC the intergovernmental panel on climate change*. Cambridge University Press.
- Taş, N., Prestat, E., McFarland, J. W., Wickland, K. P., Knight, R., Berhe, A. A., Jorgenson, T., Waldrop, M. P., & Jansson, J. K. (2014). Impact of fire on active layer and permafrost microbial communities and metagenomes in an upland Alaskan boreal forest. *ISME Journal*, 8(9), 1904–1919. <https://doi.org/10.1038/ismej.2014.36>
- Tesi, T., Muschitiello, F., Smittenberg, R. H., Jakobsson, M., Vonk, J. E., Hill, P., Andersson, A., Kirchner, N., Noormets, R., Dudarev, O., Semiletov, I., & Gustafsson, Ö. (2016). Massive remobilization of permafrost carbon during post-glacial warming. *Nature Communications*, 7, 13653. <https://doi.org/10.1038/ncomms13653>
- Walker, J. K., Egger, K. N., & Henry, G. H. (2008). Long-term experimental warming alters nitrogen-cycling communities but site factors remain the primary drivers of community structure in high arctic tundra soils. *ISME Journal*, 2(9), 982–995. <https://doi.org/10.1038/ismej.2008.52>
- Wang, Q., Garrity, G. M., Tiedje, J. M., & Cole, J. R. (2007). Naive Bayesian classifier for rapid assignment of rRNA sequences into the new bacterial taxonomy. *Applied and Environmental Microbiology*, 73(16), 5261–5267.
- Wei, S., Cui, H., Zhu, Y., Lu, Z., Pang, S., Zhang, S., Dong, H., & Su, X. (2018). Shifts of methanogenic communities in response to permafrost thaw results in rising methane emissions and soil property changes. *Extremophiles*, 22(3), 447–459. <https://doi.org/10.1007/s00792-018-1007-x>
- Woodcroft, B. J., Singleton, C. M., Boyd, J. A., Evans, P. N., Emerson, J. B., Zayed, A. A. F., & Tyson, G. W. (2018). Genome-centric view of carbon processing in thawing permafrost. *Nature*, 560(7716), 49–54.
- Wu, L., Yang, Y., Chen, S. I., Jason Shi, Z., Zhao, M., Zhu, Z., Yang, S., Qu, Y., Ma, Q., He, Z., Zhou, J., & He, Q. (2017). Microbial functional trait of rRNA operon copy numbers increases with organic levels in anaerobic digesters. *ISME Journal*, 11(12), 2874–2878. <https://doi.org/10.1038/ismej.2017.135>
- Xue, K., M. Yuan, M., J. Shi, Z., Qin, Y., Deng, Y. E., Cheng, L., Wu, L., He, Z., Van Nostrand, J. D., Bracho, R., Natali, S., Schuur, E. A. G., Luo, C., Konstantinidis, K. T., Wang, Q., Cole, J. R., Tiedje, J. M., Luo, Y., & Zhou, J. (2016). Tundra soil carbon is vulnerable to rapid microbial decomposition under climate warming. *Nature Climate Change*, 6(6), 595–600. <https://doi.org/10.1038/nclimate2940>
- Yang, Y. (2021). Emerging patterns of microbial functional traits. *Trends in Microbiology*, 29(10), 874–882. <https://doi.org/10.1016/j.tim.2021.04.004>
- Yergeau, E., Kang, S., He, Z., Zhou, J., & Kowalchuk, G. A. (2007). Functional microarray analysis of nitrogen and carbon cycling genes across an Antarctic latitudinal transect. *ISME Journal*, 1(2), 163–179. <https://doi.org/10.1038/ismej.2007.24>
- Zhou, J., Deng, Y. E., Zhang, P., Xue, K., Liang, Y., Van Nostrand, J. D., Yang, Y., He, Z., Wu, L., Stahl, D. A., Hazen, T. C., Tiedje, J. M., & Arkin, A. P. (2014). Stochasticity, succession, and environmental perturbations in a fluidic ecosystem. *Proceedings of the National Academy of Sciences of the United States of America*, 111(9), E836–E845. <https://doi.org/10.1073/pnas.1324044111>
- Zhou, J., He, Z., Yang, Y., Deng, Y., Tringe, S. G., & Alvarez-Cohen, L. (2015). High-throughput metagenomic technologies for complex microbial community analysis: Open and closed formats. *MBio*, 6(1), e02288–e2214. <https://doi.org/10.1128/mBio.02288-14>
- Zhu, Erxiong, Cao, Zhenjiao, Jia, Juan, Liu, Chengzhu, Zhang, Zhenhua, Wang, Hao, Dai, Guohua, He, Jin-Sheng, & Feng, Xiaojuan (2021). Inactive and inefficient: Warming and drought effect on microbial carbon processing in alpine grassland at depth. *Global Change Biology*, 27(10), 2241–2253. <https://doi.org/10.1111/gcb.15541>

## SUPPORTING INFORMATION

Additional supporting information may be found in the online version of the article at the publisher's website.

**How to cite this article:** Wu, L., Yang, F., Feng, J., Tao, X., Qi, Q., Wang, C., Schuur, E. A. G., Bracho, R., Huang, Y., Cole, J. R., Tiedje, J. M., & Zhou, J. (2021). Permafrost thaw with warming reduces microbial metabolic capacities in subsurface soils. *Molecular Ecology*, 00, 1–13. <https://doi.org/10.1111/mec.16319>